SAE TECHNICAL PAPER SERIES

2008-32-0028 (SAE)
20084728 (JSAE)

Knock Detection for a Large Displacement Air-Cooled V-Twin Motorcycle Engine Using In-Cylinder Ionization Signals

Nicholas M. Danne and David L.S. Hung
Visteon Corporation

Guoming G. Zhu
Michigan State University

Jay McKoskey
Polaris Industries Inc

Small Engine Technology Conference
Milwaukee, Wisconsin
September 9-11, 2008

SAE International™

400 Commonwealth Drive, Warrendale, PA 15096-0001 U.S.A. Tel: (724) 776-4841 Fax: (724) 776-0790 Web: www.sae.org

The Engineering Meetings Board has approved this paper for publication. It has successfully completed SAE's peer review process under the supervision of the session organizer. This process requires a minimum of three (3) reviews by industry experts.

All rights reserved. No part of this publication may be reproduced, stored in a retrieval system, or transmitted, in any form or by any means, electronic, mechanical, photocopying, recording, or otherwise, without the prior written permission of SAE.

For permission and licensing requests contact:

SAE Permissions
400 Commonwealth Drive
Warrendale, PA 15096-0001-USA
Email: permissions@sae.org
Tel: 724-772-4028
Fax: 724-776-3036

All SAE papers, standards, and selected books are abstracted and indexed in the Global Mobility Database.

For multiple print copies contact:

SAE Customer Service
Tel: 877-606-7323 (inside USA and Canada)
Tel: 724-776-4970 (outside USA)
Fax: 724-776-0790
Email: CustomerService@sae.org

ISSN 0148-7191
Copyright © 2008 SAE International
Copyright © 2008 SAE Japan
Positions and opinions advanced in this paper are those of the author(s) and not necessarily those of SAE. The author is solely responsible for the content of the paper. A process is available by which discussions will be printed with the paper if it is published in SAE Transactions.

Persons wishing to submit papers to be considered for presentation or publication by SAE should send the manuscript or a 300 word abstract to Secretary, Engineering Meetings Board, SAE.

2008-32-0028 (SAE) / 20084728 (JSAE)

Knock Detection for a Large Displacement Air-Cooled V-Twin Motorcycle Engine Using In-Cylinder Ionization Signals

Nicholas M. Danne and David L. S. Hung
Visteon Corporation

Guoming G. Zhu
Michigan State University

Jay McKoskey
Polaris Industries Inc

Copyright © 2008 SAE International and Copyright © 2008 SAE Japan

ABSTRACT

To obtain the maximum output power and fuel economy from an internal combustion engine, it is often necessary to detect engine knock and operate the engine at its knock limit. This paper presents the ability to detect knock using in-cylinder ionization signals on a large displacement, air-cooled, "V" twin motorcycle engine over the engine operational map. The knock detection ability of three different sensors is compared: production knock (accelerometer) sensor, in-cylinder pressure sensor, and ionization sensor. The test data shows that the ionization sensor is able to detect knock better than the production knock sensor when there is high mechanical noise present in the engine.

INTRODUCTION

The performance of a spark ignition engine, especially an air-cooled engine, is often limited by engine knock. Allowing the engine to operate in a controlled, minor, inaudible knock condition, increases engine combustion efficiency without harming the engine components. Ideally, when the MBT (minimum spark advance for the best torque) timing is limited by knock, it is desired to operate the engine as close to MBT timing as possible with some inaudible knock; in other words, to operate at borderline knock spark timing.

Knock detection methodologies which utilize an in-cylinder pressure sensor are considered to be the most accurate means of knock detection identified so far [1 and 2]. However, due to the expensive nature of the pressure sensor, it is unlikely to be adopted for large-scale production.

A typical production knock control system operates by monitoring the output of an accelerometer mounted in a suitable location on the cylinder block, and comparing the processed signal in the knock window with the signal in a noise (background) window for each cylinder. When the ratio of the signal in the knock window and noise window is greater than a calibrated value, engine knock is declared and the spark timing is retarded by an amount sufficient to eliminate knock. If no knock is detected for a specific number of cycles, the spark will be advanced gradually in small increments toward MBT timing until knock is again detected.

Saab has been in production with a system utilizing an ionization current signal to detect engine knock since 1993. Subsequently, various papers have shown the benefits of using the ionization signal to detect knock [3, 4, and 5]. Since then, knock detection based upon the ionization current signal has been accepted as an established methodology [6, 7, and 8]. Ionization current-based sensing has not been widely adopted in the automotive industry, however, despite the clearly demonstrated benefits of full-range misfire, knock detection and enhanced closed-loop combustion control [9 and 10]. One reason for the lack of adoption could be an impedance mismatch between the ignition system and the ionization detection system; the high-frequency bandwidth of ionization knock detection often requires low-inductance ignition coils, whereas engine applications requiring high-energy ignition may require high-inductance ignition coils. Other factors affect the signal-to-noise ratio of the ionization signal, and have caused it to be considered inferior to the in-cylinder pressure signal [11]. The location of the spark plug has also created doubts about knock detection for engines equipped with a centrally located spark plug [12 and 13].

An ionization detection system uses a spark plug as a sensor to monitor the in-cylinder combustion process when a bias voltage is applied between the spark plug

center and ground electrodes. Since the flame starts at the spark plug gap and gradually moves away from it, the ionization signal may contain more detailed information about in-cylinder combustion than an in-cylinder pressure signal. In fact, when the engine load is high enough, the ionization signal can be used to locate the in-cylinder pressure peak [9]. Figure 1 shows a typical ionization signal (solid line) for an air-cooled 1.7-liter two-cylinder "V" twin engine operated at 1500 RPM with 8.7 Bar IMEP (Indicated Mean Effective Pressure), alongside the corresponding in-cylinder pressure signal (dotted line). The ionization and pressure signals are 300-cycle averaged.

The typical ionization signal has two peaks. The first peak is due to the initial flame kernel development immediately following the spark. When the flame front leaves the spark plug, the magnitude of the ionization signal is reduced. As the pressure in the cylinder increases rapidly, the combusted mixture around the spark plug gap is ionized again due to the high temperature resulting from the combustion, which generates the second peak. For water-cooled engines, the second peak is co-located with the peak in-cylinder pressure signal [9], but for this air-cooled engine there is an offset of $\Delta\theta$ angle. That is, the peak cylinder pressure location is retarded from the second peak location of the ionization signal by $\Delta\theta$ amount.

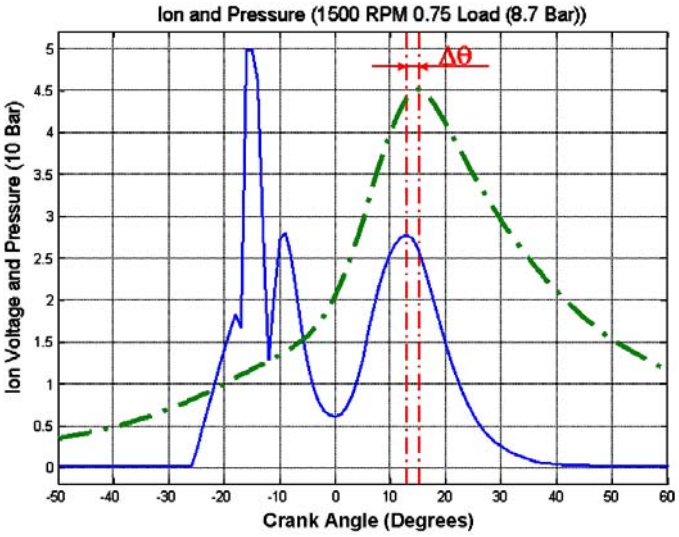

Figure 1: Ionization signal from an air-cooled engine

Figure 2 shows 300-cycle averaged ionization and pressure signals at different speed and load conditions, where the dotted line is in-cylinder pressure and the solid line is the ionization signal. It is worth mentioning that at high engine speed, the first peak of the ionization signal disappears since it is covered by the spark pulse. The second peak of the ionization signal, however, is strong for all conditions, which is important for knock detection.

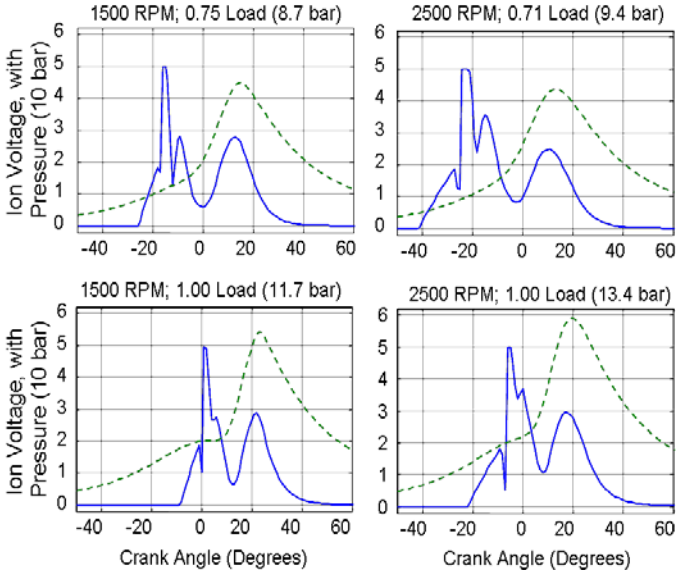

Figure 2: Ionization Signals Over Engine Map

For a motorcycle, the air-cooled engine is often integrated with the transmission gear box, which introduces additional mechanical vibration noise to the engine. This makes it difficult to use a vibration-based knock senor for engine knock detection, especially, at high engine speed when engine and transmission vibrations become dominant. We propose to use the ionization signal as an alternative low-cost knock sensor that is immune to unwanted mechanical noise.

Compared to the conventional water-cooled automotive engine, air-cooled engines typically exhibit a much wider range of cylinder head temperature, including a higher peak temperature. Furthermore, the V-twin engine contains two cylinders in a "V" configuration, with one cylinder positioned in front of the other. In this configuration, the circulation of ambient air streams around the exterior of each cylinder is estimated to be non-uniform [14], with an estimated higher running temperature in the rear cylinder for most operating conditions. Due to these characteristics of the engine, it was hypothesized that the rear cylinder would be more susceptible to knock than the front cylinder.

The objective of this paper is to investigate the capability of ionization sensing to detect knock in an air-cooled motorcycle engine. The paper is organized as follows: The Experimental Setup And Data Analysis section describes the specific test equipment used for the engine testing, the data acquisition method, the engine test matrix, the knock intensity calculation, and equations defining the correlation of knock intensity between different sensor types. The Discussion section focuses on three key points of this investigation and will be presented in detail: ionization knock detection and characteristics for an air-cooled engine, correlation between pressure and ionization knock intensities, and correlation between pressure and accelerometer knock intensities. Finally, the applicability of ionization knock detection for air-cooled engines is discussed.

EXPERIMENTAL SETUP AND DATA ANALYSIS

The test data shown in this paper was obtained using an air-cooled 1.7-liter two-cylinder "V" twin engine (see Figure 3) equipped with a conventional Port-Fuel-Injection (PFI) fuel system. The PFI rail pressure was regulated at 3.5 bar. The cylinder head was instrumented with a laboratory-grade pressure sensor, and a UEGO (universal exhaust gas oxygen) sensor was installed for air-to-fuel ratio measurement and control. The ionization detection system used for the test was an ionization detection ignition coil with integrated electronics and coil driver. The integrated coil was a coil-on-plug design. Each cylinder block was instrumented with a conventional knock sensor (accelerometer) from a production vehicle. Optimization of the accelerometer location was not performed in this experiment.

The "V" twin engine was controlled by a prototype engine controller for spark timing and fuel injection, and the engine throttle and speed were regulated by the engine dynamometer controller. Exhaust-Gas-Recirculation (EGR) was not used for any of the tests. A cooling fan was placed in front of the engine (cylinder #1) to mimic the air streams which traverse the cylinders during a motorcycle driving condition.

Figure 3: Air-cooled "V" twin test engine

In-cylinder pressure and air-to-fuel ratio signals were collected using a dynamometer data sampling system with one crank degree of resolution. For each test case, 300 cycles of data were collected with one crank degree of resolution. For knock-related tests, a 4-second duration signal was collected at 100 kHz sample rate. The engine air-to-fuel ratio was selected based upon the actual engine operational requirement. The engine was set to borderline (BDL) spark timing, and spark timing sweeps were conducted at BDL, BDL ±2, and BDL ±4 degrees.

Figure 4 shows the test matrix of operating points where the engine was knock-limited (solid blocks; 1500 to 2000 RPM at 75% to 100% load, and 2500 RPM at 85% to 100% load), borderline knock-limited (horizontal bar blocks; 2500 RPM at 75% load and 3000 RPM at 75% to 100% load), or where MBT timing was not limited by knock (vertical bar blocks; 50% load for all speeds, and all loads at 3500 RPM or higher). This study is focused on the operational conditions where the engine is knock-limited.

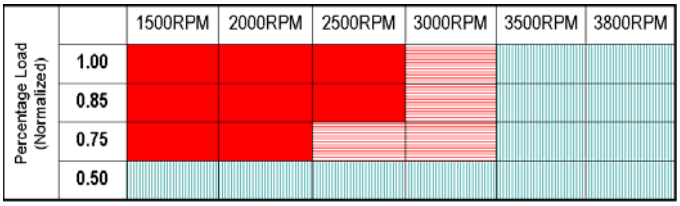

Figure 4: Test matrix

When an engine is operated at knock conditions, there exist high frequency oscillations superimposed on the ionization signal after the second peak (see Figure 6). A knock intensity signal can be obtained using a conventional accelerometer knock sensor, an in-cylinder pressure sensor, or an ionization sensor. For this paper, knock intensity is defined as the integration, over a defined knock window, of the absolute value of the bandpass-filtered knock signal obtained from any of the three sensor types (see Figure 5). The knock window was selected to begin at the location of peak cylinder pressure, and was given a duration of 20 crank-angle degrees. The bandpass filter used for data analysis was an eight-pole Butterworth filter with corner frequencies at 2 kHz and 15 kHz.

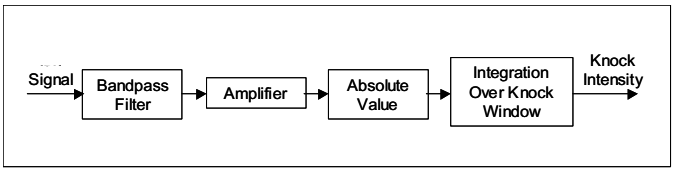

Figure 5: Knock intensity calculation diagram

Equations 1 through 5 define the correlation of knock intensities between different sensor types. In equation 1, knock intensity matrix Y is defined as three vertical vectors, I_{ION}, I_P, and I_{KS}, which represent the ionization knock intensity vector, the pressure knock intensity vector, and the accelerometer knock intensity vector, respectively. Each knock intensity vector has a length equal to the number of firing events in the aforementioned 4-second sampling period.

$$Y = \begin{bmatrix} I_{ION} & I_P & I_{KS} \end{bmatrix} \quad (1)$$

Per equation 2, knock intensity mean matrix Y_m consists of vectors $I_{ION\text{-}MN}$, $I_{P\text{-}MN}$, and $I_{KS\text{-}MN}$, which are equal in size to I_{ION}, I_P, and I_{KS}, respectively. Each element of

vector I_{ION-MN}, I_{P-MN}, and I_{KS-MN} equals the mean of its corresponding vector in *Y*.

$$Y_m = \begin{bmatrix} I_{ION-MN} & I_{P-MN} & I_{KS-MN} \end{bmatrix} \quad (2)$$

Matrix *R* is defined in equation 3. Notice that *R* is a positive definite matrix, proportional to the covariance matrix of *Y*. Therefore, $R(i,i) > 0, \mathrm{i} = 1,2,3$ if the individual vectors of I_{ION}, I_P, and I_{KS} are not zero.

$$R = \left(Y - Y_m\right)^T \left(Y - Y_m\right) \quad (3)$$

Matrix $\overline{R}$ is defined as follows:

$$\overline{R}(i,j) = \begin{cases} \sqrt{R(i,j)} & for \quad i = j = 1, 2, 3 \\ 0 & for \quad i \neq j \end{cases} \quad (4)$$

Finally, the knock intensity correlation matrix is obtained by normalizing matrix *R*, as shown in equation 5.

$$Corr = \overline{R}^{-1} \bullet R \overline{R}^{-1} \quad (5)$$

DISCUSSION

IONIZATION KNOCK DETECTION FOR AN AIR-COOLED ENGINE

Figure 6 compares the ionization and in-cylinder pressure signals at 1500 RPM and 85% load, with timing 4 degrees advanced from BDL. The top graph shows the raw ionization and in-cylinder pressure signals, and the bottom graph shows the bandpass-filtered version of those signals, with low-frequency content reduced and the knock frequency amplified. The knock window is represented by the dotted lines. It is obvious that the engine experienced a relatively high level of knocking at this operating condition, as indicated by the amplitude of the high-frequency component of both the ionization and pressure signals. As expected, there is a strong correlation between these two knock intensities over 50 engine cycles; the correlation value is 0.8777. It can also be observed that the peak-to-peak filtered pressure was approximately 18 bar. This indicates heavy knocking in the engine, since borderline knock was measured to be approximately 1.4 bar.

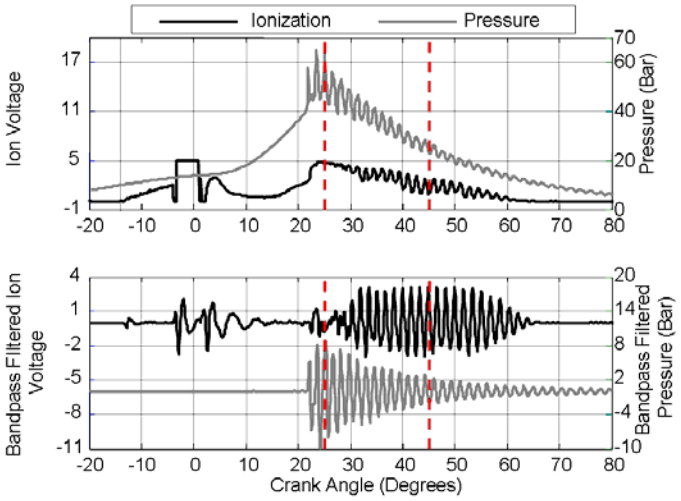

Figure 6: Heavy knock ionization and pressure signals, with knock window

Figure 7 depicts borderline knock. The test condition was 1500 RPM with 85% load at BDL spark timing. Since the spark timing was retarded by 4 degrees from the previous test, the engine experienced significantly less knocking. The ionization and pressure signals show the reduced knocking intensities and correlate strongly to each other. The knock intensity correlation for these two signals, over 50 engine cycles, is 0.8939.

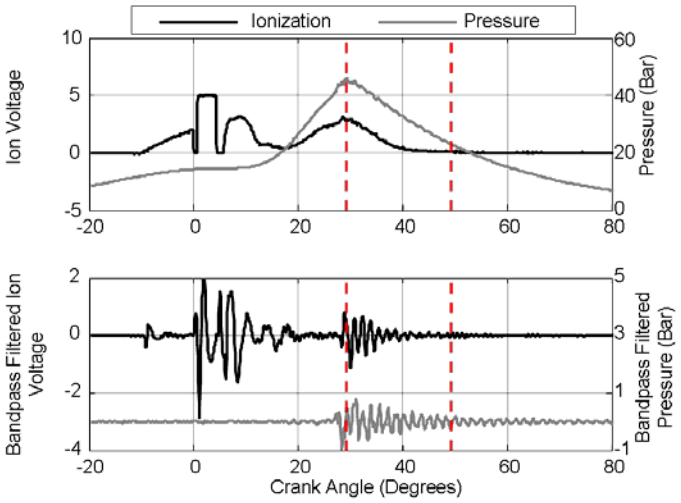

Figure 7: Borderline knock ionization and pressure signals, with knock window

The characteristics of ionization signals were found to be similar between an air-cooled engine and water-cooled engines [7]. As described earlier in this paper, the second peak of the ionization signal is generated by re-ionization of the combusted mixture in the vicinity of the spark plug, due to the high temperature of the combustion event. Since air-cooled engines typically run hotter than water-cooled engines, the second peak of the ionization signal on an air-cooled engine is expected to be of greater amplitude than that for a water-cooled

engine. Thus the ionization signal in an air-cooled engine is expected to have a higher sensitivity to engine knock than in a water-cooled configuration.

Figure 8 illustrates the sensitivity of ionization to changes in spark advance for an air-cooled engine. Operating at 1500 RPM and 85% load, the instantaneous pressure and ionization amplitudes are small for the spark timing of 2 degrees retarded from BDL. As spark timing is advanced by 2 degrees to reach the BDL, the instantaneous pressure and ionization amplitudes increase. Further increasing the spark timing to 2 degrees advanced of BDL, the instantaneous pressure and ionization amplitudes increase dramatically. Finally, as the spark timing is increased to a total of 4 degrees advanced from BDL, the instantaneous pressure and ionization amplitudes are large, indicating that the engine is experiencing heavy knock. This demonstrates that ionization responds to an increase in spark advance with a change in amplitude comparable to the change in amplitude of the pressure signal.

Of interest is the more rapid attenuation of the ionization knock signal than the pressure signal over time; this is primarily due to the temperature reduction that occurs in the cylinder when the piston moves away from TDC. Because the ionization knock signal relies on thermal ionization, which is heavily temperature-dependent, its amplitude decreases more rapidly than that of the pressure knock signal, which is based on the pressure wave generated by irregular knock combustion and is independent of in-cylinder temperature. Nonetheless, correlations between ionization and pressure knock intensities remain high over a 50-cycle average for the same knock window; in this case, correlations ranged from 0.7269 to 0.8939, all considered to be acceptable values.

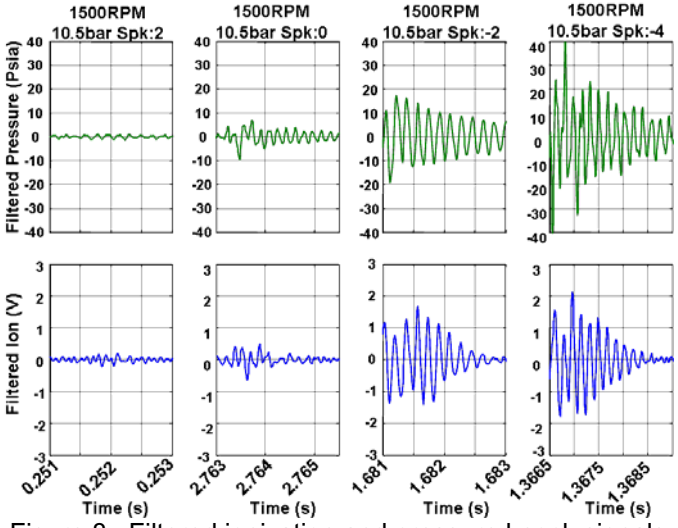

Figure 8: Filtered ionization and pressure knock signals

CORRELATION BETWEEN IONIZATION KNOCK SIGNAL AND PRESSURE KNOCK SIGNAL

Figure 9 illustrates the heavily-knocking case of 1500 RPM and part-load (85%) at 4 degrees advanced from BDL. As can be seen in the graph, the ionization and pressure knock intensities track each other on a cycle-to-cycle basis; for example, cycle 30 exhibits the highest calculated knock intensity for both ionization and pressure, whereas cycles 9 and 10 are in each case low-intensity compared to their peers. This suggests a strong correlation of knock intensity between ionization and pressure over consecutive engine cycles.

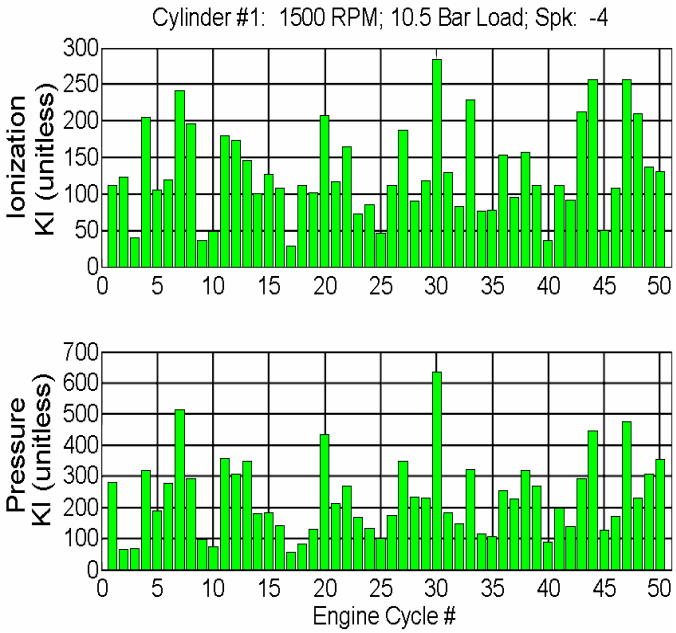

Figure 9: Knock Intensity by Engine Cycle

The data in Figure 9 was re-displayed in Figure 10 to illustrate the linear regression between ionization and pressure knock intensities. Figure 10 shows that each data point remains relatively close to the trend line, suggesting that increases in pressure knock intensity correlate to increases in ionization knock intensity. The R^2 value for this linear regression was 0.7706.

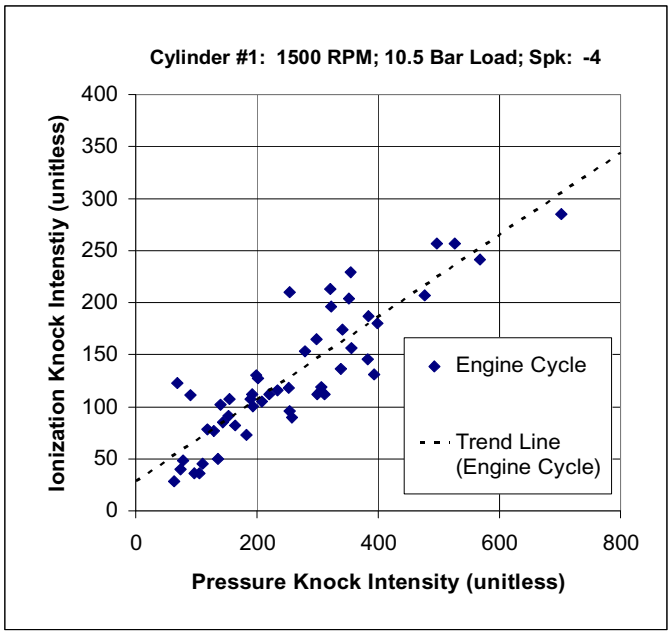

Figure 10: Knock Intensity Trend Line

Table 1 shows a strong correlation between ionization and pressure knock intensities over the operating range of interest, specifically the knock-limited conditions of 1500 to 3000 RPM and 75% to 100% load. It is noted that the correlation between ionization and pressure knock intensities remains greater than 0.80 for all loads at 1500 RPM, as well as for all speeds at wide-open-throttle (100% load). The correlation between ionization and pressure knock intensities is greater than 0.72 for the engine operating range of interest.

Table 1: Knock intensity correlation (ion and pressure)

	Percentage Load		
RPM	75%	85%	100%
1500	0.8199	0.8777	0.8485
2000	0.8712	0.7626	0.9603
2500	0.7286	0.8661	0.8864
3000	0.7631	0.8881	0.8267

Correlation between ionization and pressure knock intensities is also illustrated in Figure 11 and Figure 12. For discrete RPM's at 85% load, and for 2000 RPM at 100% load, the ionization and pressure knock intensities increase for each advance in spark timing. This suggests an excellent correlation between pressure and ionization in each individual cylinder.

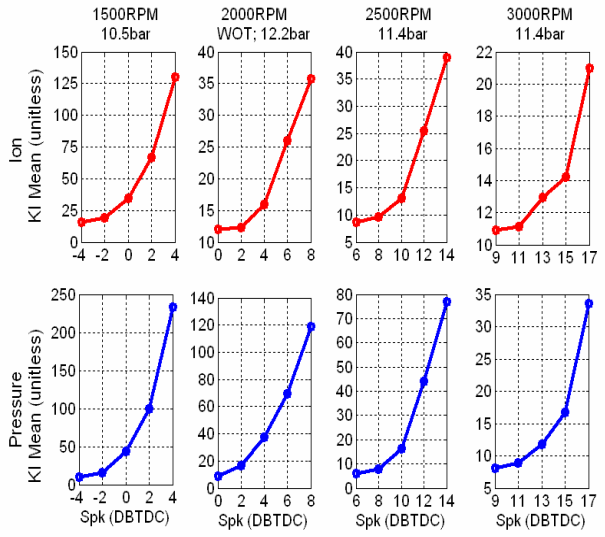

Figure 11: Four Instances of Knock, Cylinder #1

Of interest are the differences in pressure knock intensity between cylinders #1 and #2, and the corresponding difference in ionization knock intensity. For example, the 2000 RPM case at 6 degrees advanced from TDC exhibits a pressure knock intensity of approximately 70 (unitless) in cylinder #1, and 32 in cylinder #2. The ionization knock intensities follow this trend, with values of approximately 26 (unitless) and 14, respectively.

Conversely, in the 2500 RPM case at 12 degrees advanced from TDC, cylinder #2 exhibits a pressure knock intensity of approximately 65, while cylinder #1 exhibits a pressure knock intensity of approximately 45. In this case, cylinder #2 exhibits higher pressure knock intensity than cylinder #1, and ionization follows this trend, as can be seen from the graphs.

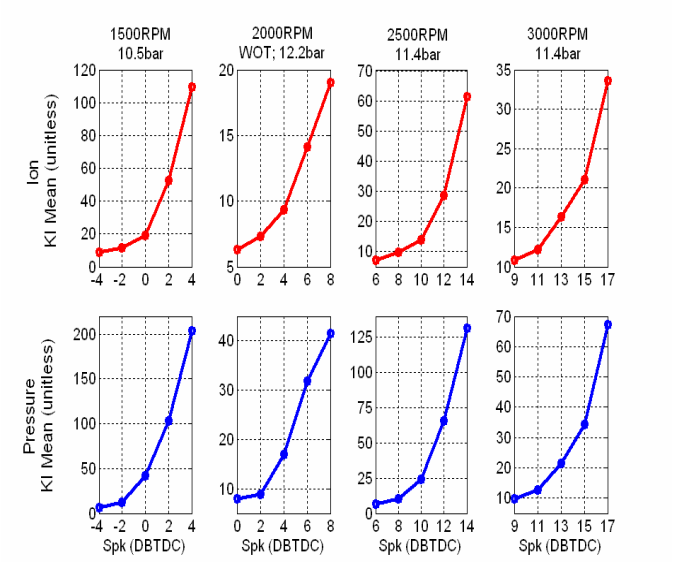

Figure 12: Four Instances of Knock, Cylinder #2

The cylinder-to-cylinder difference in knock intensity for Figures 11 and 12 is illustrated in Figure 13. Figure 13 plots, for a given RPM, the subtraction of knock intensity of cylinder #2 from the knock intensity of cylinder #1, averaged over five spark advances, and normalized to the average knock intensity of the two cylinders at all spark advances. It is observed from Figure 13 that for test conditions less than or equal to 2000 RPM, cylinder #1 tends to exhibit higher pressure and ionization knock intensities than cylinder #2, but for test conditions greater than or equal to 2500 RPM, cylinder #2 tends to exhibit higher pressure and ionization knock intensities than cylinder #1.

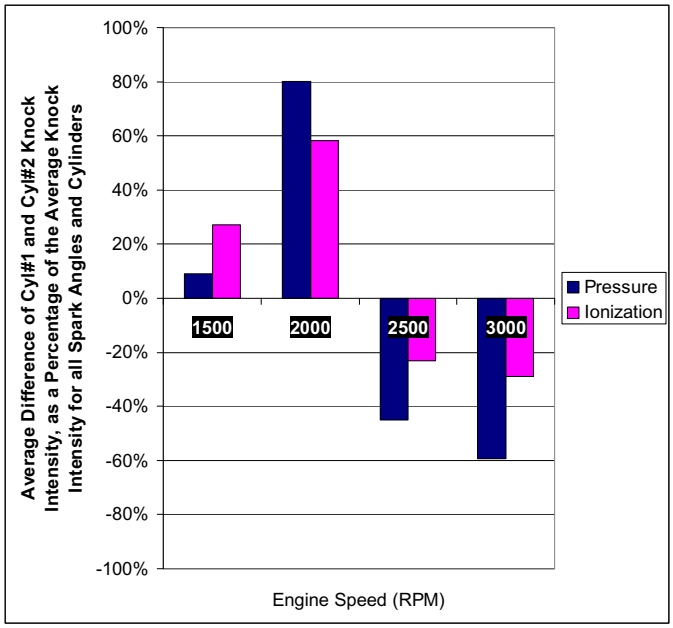

Figure 13: Cylinder-to-Cylinder Knock Intensity

Figures 11 through 13 indicate that differences in pressure between cylinder #1 and cylinder #2 are not uniform over all engine speeds and loads, and also do not support the hypothesis that the rear cylinder (#2) would exhibit higher pressures and be more prone to knock at every operating condition. We believe that this cylinder-to-cylinder knock intensity dependence on RPM is mainly due to variations in the intake air charge at different engine speeds, which leads to relative load variation for individual cylinders, even though the individual cylinder air-to-fuel ratio was kept constant.

CORRELATION BETWEEN PRESSURE KNOCK SIGNAL AND KNOCK SENSOR SIGNAL

The conventional method of knock detection is by way of an engine-mounted accelerometer, calibrated to pass knocking frequencies and to reject ambient vibrations. In practice, however, mechanical noise from the engine may corrupt the ability of an accelerometer to detect knock at high engine RPM.

Ionization sensors may be used to substitute noise-crippled accelerometers, especially in the detection of inaudible or borderline knock. Figure 14 illustrates the difference in sensor correlations during heavy knock (4 degrees advanced from BDL) as opposed to inaudible knock (4 degrees retarded from BDL). It is observed that the correlation between ionization and pressure sensors for both heavy and inaudible knock is strong, but for this speed-load condition (3000 RPM, 100% load), the correlation between accelerometer and pressure decreases dramatically from the heavy knock to the inaudible knock case. This suggests that the accelerometer is not dependable for detecting inaudible knock, whereas the ionization signal detects inaudible knock accurately under mechanically noisy conditions. Detection of inaudible knock is important for improving existing knock control capability [7].

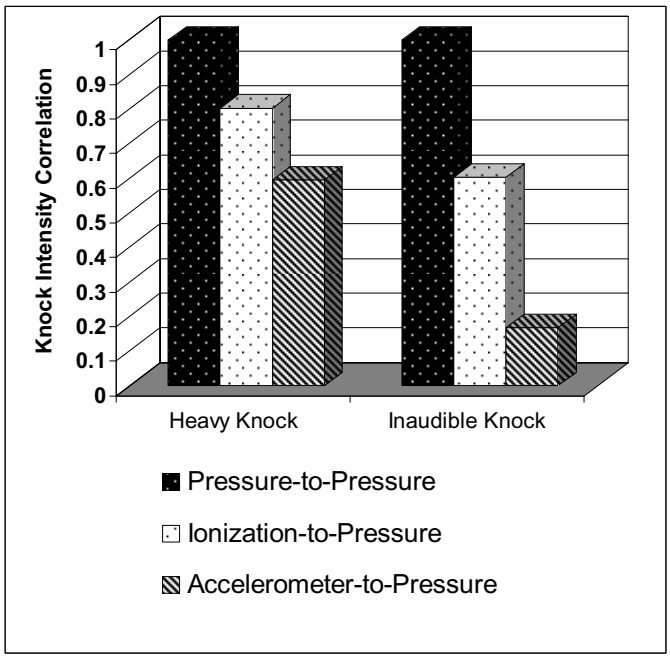

Figure 14: Correlation Differences between Heavy Knock and Inaudible Knock

The deficiency of the accelerometer in knock detection is also illustrated in Figure 15. The operating condition is 3000 RPM at 100% load, with spark timing of 2 degrees retarded from BDL. As can be seen in the top graph, the band-pass filtered accelerometer signal does not peak in the same locations as the filtered pressure signal peaks. This suggests a low or unreliable correlation. In the bottom graph, there appears to be little response from the accelerometer during high pressure peaks, compared to the background noise. Although correlation between the accelerometer and pressure knock intensities in this case was 0.4379, the difference between pressure and accelerometer signal amplitudes in Figure 15 suggests that this value of correlation is insufficient at high RPM and load. Correlation between ionization and pressure knock intensities for this case was 0.6677.

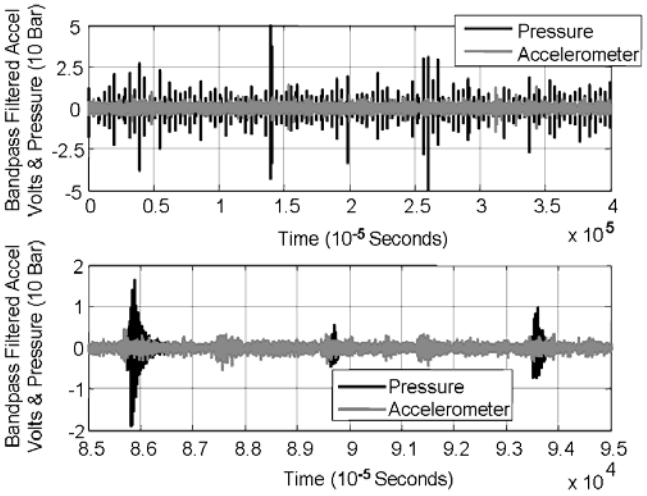

Figure 15: Accelerometer Deficiency at High RPM

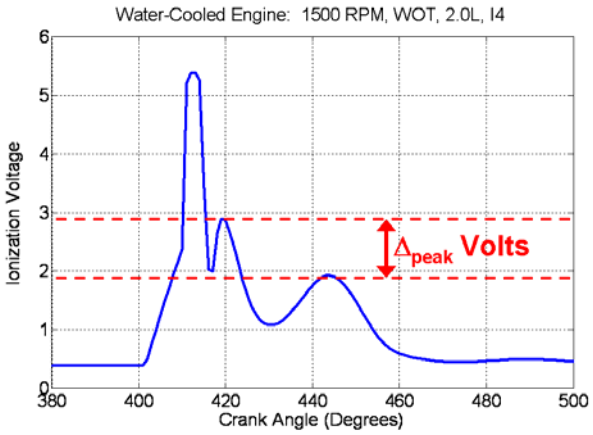

Figure 16: Ionization Signal from a Water-Cooled Engine

FURTHER DISCUSSION

The need for individual cylinder knock detection and control in motorcycle engines has been suggested [15]. This study shows that ionization knock detection is able to provide individual cylinder knock control on an air-cooled motorcycle engine. Referring again to Figures 11 through 13, it has been shown that to calibrate both cylinders to provide equal spark retard, or to assume that one cylinder will always need greater spark retard, is not practical. In particular, Figure 13 illustrates that engine speed influences individual cylinder knock intensity. Considering the sensitivity of the ionization signal to knock intensity as a function of spark advance, coupled with the varying dominance of pressure knock intensity between cylinders, it appears that the air-cooled engine would be a suitable candidate for an ionization-based stochastic knock control system [9].

Also of interest is the difference in ionization signal profile between air-cooled and water-cooled engines. Figure 16 shows a 100-cycle averaged ionization signal for a 2.0L displacement, water-cooled I4 engine operated at 1500 RPM and WOT load. From the plot there can be seen a difference of Δ_{peak} volts between the first and second ionization peaks. In contrast, returning to the air-cooled ionization signal of Figure 1, also at 1500 RPM but at light load (75%), the air-cooled ionization signal yields almost identical amplitudes of first and second ionization peaks. Due to the higher running temperature of air-cooled engines, the amplitude of the second peak of the ionization signal is generally greater than in water-cooled engines, yielding a higher sensitivity to knock and an estimated increase in reliability for knock detection and control.

CONCLUSION

Knock detection capability via ionization sensing on a large-displacement, air-cooled, V-twin motorcycle engine was demonstrated in this study. Ionization knock detection was also compared to the conventional methods of pressure-based and accelerometer-based knock detection. Strong correlations were found between the ionization and pressure knock intensities for both the heavy knocking and inaudible knocking cases. These correlation values were greater than the correlations calculated between pressure and accelerometer knock intensities in the inaudible knock range.

Ionization knock detection is shown to be a viable alternative to accelerometer-based knock detection on large displacement, air-cooled motorcycle engines. In addition, ionization sensing is capable of detecting inaudible knock more accurately and rejecting mechanical noise more effectively than the conventional accelerometer-based knock sensor. There exists a strong correlation between ionization and pressure knock intensities for the knock-limited operating range of interest.

ACKNOWLEDGMENTS

The authors would like to acknowledge Kurt Hesse of Visteon Corporation, and Polaris Industries Inc, for providing program support in this investigation.

REFERENCES

1. S. Diana, V. Giglio, B. Lorio, and G. Police, “Evaluation of the effect of EGR on engine knock,” *SAE 982479*, 1998.
2. R. Worret, S. Bernhardt, F. Schwarz, and U. Spicher, “Application of different cylinder pressure based knock detection methods in spark ignition engines,” *SAE 2002-01-1668*, 2002.
3. J. Auzins, H. Johansson, and J. Nytomt, “Ion-gap sense in misfire detection, knock and engine control,” *SAE 950004*, 1995.
4. Y. Ohashi, W. Fukui, and A. Ueda, “Application of vehicle equipped with ionic current detection system for the engine management system,” *SAE 970032*, 1997.
5. Y. Ohashi, W. Fukui, F. Tanabe, and A. Ueda, “The application of ionic current detection system for the combustion limit control,” *SAE 980171*, 1998.
6. A. Saitzkoff, R. Reinmann, and F. Mauss, “In-cylinder pressure measurements using the spark plug as an ionization sensor,” *SAE 970857*, 1997
7. C. F. Daniels, G. G. Zhu, J. Winkelman, “Inaudible knock and partial burn detection using in-cylinder ionization signals,” *SAE 2003-01-3149*, 2003.
8. G. W. Malaczynski and M. E. Baker, “Real-time digital signal processing of ionization current for engine diagnostics and control,” *SAE 2003-01-1119*, 2003.
9. G. G. Zhu, I. Haskara, J. Winkelman, “Closed loop ignition timing control using ionization current feedback,“ *IEEE Transaction on Control System Technology,* May, 2007.
10. L. Eriksson and L. L. Nielsen, “Closed loop ignition control by ionization current interpretation,” *SAE 970854,* 1997.
11. L. Peron, A. Charlet, P. Higelin, B. Moreau, and J. F. Burq, “Limitations of ionization current sensors and comparison with cylinder pressure sensors,” *SAE 2000-01-2830*, 2000.
12. S. Byttner, T.S. Rognvaldsson, and N. Wickstrom, “Estimation of combustion variability using in-cylinder ionization measurements,” *SAE 2001-01-3485*, 2001.
13. D. Scholl, C. Davis, S. Russ, and T. Barash, “The volume acoustic modes of spark ignited internal combustion chambers,” *SAE 980893*, 1998.
14. Y. Takahashi and Y. Gokan, “CFD Analysis of Air Flow of Air-Cooled Motorcycle Engines,” SAE 2006-32-0005, 2006.
15. Wade, Adam (2004). *Motorcycle Fuel Injection Handbook*. St. Paul: Motorbooks International. p94.

CONTACT

Nicholas Danne, Visteon Corporation, One Village Center Drive, Van Buren Township, MI 48111, USA. E-mail: ndanne@visteon.com (734-710-4515)

DEFINITIONS, ACRONYMS, ABBREVIATIONS

Accel:	Accelerometer
BDL:	Borderline
Cyl:	Cylinder
DBTDC:	Degrees Before Top Dead Center
EGR:	Exhaust-Gas-Recirculation
I4:	Inline, four-cylinder engine
IMEP:	Indicated Mean Effective Pressure
ION:	Ionization
kHz:	Kilohertz
KI:	Knock Intensity
L:	Liters
MBT:	Minimum spark advance for Best Torque
PFI:	Port Fuel Injection
Psia:	Pounds-force per square inch absolute
RPM:	Revolutions Per Minute
s:	Seconds
Spk:	Spark timing (retarded from BDL unless otherwise indicated)
TDC:	Top Dead Center
UEGO:	Universal Exhaust Gas Oxygen
V:	Volts
WOT:	Wide Open Throttle